



Thermomechanical response of porous biological tissue based on local thermal non-equilibrium

Xiaoya Li, Qing-Hua Qin & Xiaogeng Tian

To cite this article: Xiaoya Li, Qing-Hua Qin & Xiaogeng Tian (2019) Thermomechanical response of porous biological tissue based on local thermal non-equilibrium, Journal of Thermal Stresses, 42:12, 1481-1498, DOI: [10.1080/01495739.2019.1660599](https://doi.org/10.1080/01495739.2019.1660599)

To link to this article: <https://doi.org/10.1080/01495739.2019.1660599>



Published online: 15 Oct 2019.



Submit your article to this journal [↗](#)



Article views: 24



View related articles [↗](#)



View Crossmark data [↗](#)



Thermomechanical response of porous biological tissue based on local thermal non-equilibrium

Xiaoya Li^{a,b}, Qing-Hua Qin^b, and Xiaogeng Tian^a

^aState Key Laboratory for Strength and Vibration of Mechanical Structures, Shaanxi Engineering Research Center of Nondestructive Testing and Structural Integrity Evaluation, School of Aerospace, Xi'an Jiaotong University, Xi'an, PR China; ^bResearch School of Engineering, College of Engineering and Computer Science, Australian National University, Acton, ACT, Australia

ABSTRACT

Understanding of heat transfer and related thermomechanical interaction in biological tissue is very important to clinical applications. It is quite natural to treat the living tissue as a porous medium, such as the living tissue in the presence of blood. Based on a non-equilibrium heat transfer model, the thermomechanical response of porous biological tissue exposed to an instantaneous thermal shock is investigated in this work. The governing equations are established based on local thermal non-equilibrium model in the context of the generalized thermoelastic theory and solved by time-domain finite-element method. The effect of porosity coefficient on the thermal-mechanical response of the porous tissue is studied and illustrated graphically. Comparisons are made between the proposed results and those from the local thermal equilibrium models to reveal the difference of these two models in terms of thermoelastic response.

ARTICLE HISTORY

Received 21 August 2018
Accepted 9 April 2019

KEYWORDS

Local thermal non-equilibrium; generalized thermoelastic theory; finite-element method; porosity coefficient

1. Introduction

Analysis of heat transfer in biological tissue is a complicated physiological process including heat conduction in tissue, convective between blood and vessel, and blood perfusion. The biological tissue consists of cell and micro-vascular bed with the blood flow through many vessels. Thus, it can be treated as a porous media and divided into vascular region and extravascular region. Studies on heat transfer in porous media are generally based on two different models: local thermal equilibrium (LTE) and local thermal non-equilibrium (LTNE). Many previous studies have investigated bioheat transfer problem based on the LTE model [1]–[4], where the temperature of tissue and blood is equal everywhere in this model. This assumption holds true when heat exchange between tissue and blood are efficient. It is, in general, valid only in a capillary bed that has many micro-vessels (of small diameter) and a large area of heat transfer [5]. Khaled and Vafai [6] presented a review on the role of porous media in modeling flow and heat transfer in biological tissue. They indicated that developing advanced heat transfer models according to the thermal non-equilibrium state between blood and tissue is important.

Based on the non-equilibrium heat transfer model, Zhang [7] established a generalized dual-phase lag bioheat equation. Fan and Wang [8] developed a general bioheat transfer model at macro-scale for biological tissue, which also showed both the temperature of tissue and blood is

CONTACT Xiaogeng Tian  tiansu@mail.xjtu.edu.cn  State Key Laboratory for Strength and Vibration of Mechanical Structures, Shaanxi Engineering Research Center of Nondestructive Testing and Structural Integrity Evaluation, School of Aerospace, Xi'an Jiaotong University, Xi'an, 710049, PR China.

Color versions of one or more of the figures in the article can be found online at www.tandfonline.com/uths.

satisfied with dual-phase lag energy equation. Afrin et al. [9] presented a thermal lagging model in biological tissue between tissue, arterial and venous bloods. They found that the phase lag times are dependent on the material properties of tissue and blood. But the above-mentioned studies all assumed the blood temperature undergone a transient process and it was a function of tissue temperature [7]–[9]. This assumption may not be used to predict the real temperature of blood and tissue. To bypass this problem, Xuan and Roetzel [10] established three energy equations based on the concept of porous media and obtained the steady temperature distributions of tissue, artery, and vein. Then, Roetzel and Xuan [11] investigated the transient heat transfer problem between the artery, vein, and tissue in a cylinder physical model. Mahjoob and Vafai [12] obtained the exact solutions of the tissue and blood temperature profiles in hyperthermia treatment. An equivalent heat transfer coefficient between tissue and blood in a porous model for simulating the biological tissue in a hyperthermia therapy based on the LTNE model was investigated by Yuan [13]. He indicated that the equivalent heat transfer coefficient was inversely related to the blood vessel diameter. Belmiloudi [14] analyzed the temperature distribution in bio-fluid heat transfer of porous non-homogeneous tissues during thermal therapy based on the LTNE model.

It is noted that even a small change of heat-induced stress can suppress immune response, alter production of hormones and protein denaturation [15]. The thermoelastic effect also relates to the thermal damage such as tissue shrinkage. The blood flow has an important effect on the deformation. However, only few studies focus on thermomechanical interaction of porous biological tissue subjected to thermal shock based on the LTNE model, even if there are studies of thermomechanical interaction limited to the LTE model or regard biological tissue as a continuous model [16, 17]. Thermal stress-related LTNE model has been addressed in a few studies [18]–[21]. But the heat conduction equations in these studies are all based on Fourier's law, which predict an infinite speed of propagation for heat conduction. It is well known that heat travels at a finite speed in particular heat treatment conditions, i.e. high-power with short durations and cryogenic temperature, or heat conduction in media with non-homogeneous inner structure. To eliminate such paradox, two generalized thermoelastic theories established by Lord and Shulman [22] and Green and Lindsay [23], which predict thermal signal propagates with a finite speed. They have been widely used to investigate transient thermal shock problems.

In this study, we investigate the transient coupled thermomechanical response of porous biological tissue using the LTNE model in the context of generalized thermoelastic theory. Comparisons are presented between LTNE and LTE models to identify the difference of these two models on the thermoelastic response. The finite-element governing equations are established in the generalized porous thermoelastic theory and solved in time-domain. The effect of porosity coefficient on the response is also illustrated graphically.

2. Problem formulation

2.1. Basic equations

It is assumed that biological tissue is linear, homogeneous and isotropically thermoelastic in the present work. No phase change and no chemical reactions occur within the biological tissue. Based on the LTNE model, the thermoelastic equations in the context of generalized thermoelastic theory can be expressed as follows (in the absence of body force):

- a. Heat conduction equations of blood and tissue

$$q_i^b = -nk^b \theta_{,i}^b + n\rho^b c^b \theta^b \dot{w}_i \quad (1)$$

$$q_i^t = -(1 - n)k^t\theta^t_{,i} \tag{2}$$

where q_i^b and q_i^t are the heat flux vectors of blood fluid and solid tissue, respectively; and $i = 1, 2, 3$; k^b and k^t are the blood and tissue thermal conductivity; ρ^b and ρ^t are the densities of blood and tissue, c^b and c^t are the specific heat for blood and tissue; θ^b and θ^t are the blood and tissue temperature increment, and $\theta^b = T^b - T_0$, $\theta^t = T^t - T_0$, $|\theta^b/T_0| \ll 1$, $|\theta^t/T_0| \ll 1$, T^b and T^t are the temperature of blood and tissue, respectively; T_0 is the reference temperature; n is porosity coefficient; w_i is blood displacement with respect to the tissue. The term of $n\rho^b c^b \theta^b \dot{w}_i$ denotes the convection effect of blood. Besides, super-dot refers to the derivative with respect to time; a comma followed by sub-index denotes the corresponding partial differentiation in this study. It is also agreed that if there is a pair of identical indicators in an item, it is considered to be the summation of this indicator.

b. The equations of energy conservation in blood and tissue

$$q_{i,i}^b = -\rho^b T_0 \dot{S}^b - ha(T^b - T^t) - \rho^b \varpi^b c^b (T^b - T^t) + nQ^{ext} \tag{3}$$

$$q_{i,i}^t = -\rho^t T_0 \dot{S}^t - ha(T^t - T^b) - \rho^b \varpi^b c^b (T^t - T^b) + (1 - n)Q^{met} + (1 - n)Q^{ext} \tag{4}$$

where S^b and S^t are the blood and tissue entropy density, respectively; ϖ^b is blood perfusion rate; h is the blood-tissue interface heat transfer coefficient; a is the specific area of the blood vessel; Q^{met} is metabolic heat; Q^{ext} is the external heat source supplied by laser. And the coupled terms of $ha(T^b - T^t)$ and $\rho^b \varpi^b c^b (T^b - T^t)$ denote interfacial convective heat transfer and blood perfusion heat conduction, respectively.

c. The modified Darcy law in fluid [24]

$$p_{,i} = -\left(\dot{w}_i/\kappa + (\rho^b/n)\ddot{w}_i + \rho^b \ddot{u}_i\right) \tag{5}$$

where u_i and p are the tissue displacement vector and excess pore pressure; $\kappa = k^l/(\rho^b g)$, k^b is the intrinsic permeability, g is the gravitational acceleration.

d. The equation of motion

$$\sigma_{ij,j} = \rho \ddot{u}_i + \rho^b \ddot{w}_i \tag{6}$$

where σ_{ij} is the stress tensor, $j = 1, 2, 3$; ρ is the effect density and $\rho = n\rho^b + (1 - n)\rho^t$.

e. The constitutive equation

$$\sigma_{ij} = 2\mu\varepsilon_{ij} + \lambda\varepsilon_{kk}\delta_{ij} - \gamma(\theta^{ave} + \tau_1\dot{\theta}^{ave})\delta_{ij} - \alpha p\delta_{ij} \tag{7}$$

$$p = M\left(a^u(\theta^{ave} + \tau_1\dot{\theta}^{ave}) - \alpha\varepsilon_{kk} + \xi\right) \tag{8}$$

$$\rho^b S^b = \frac{n\rho^b c^b}{T_0}(\theta^b + \tau_2\dot{\theta}^b) + \gamma^t \varepsilon_{kk} + \gamma^b \xi \tag{9}$$

$$\rho^t S^t = \frac{1-n}{T_0}\rho^t c^t(\theta^t + \tau_2\dot{\theta}^t) + \gamma^t \varepsilon_{kk} + \gamma^b \xi \tag{10}$$

where θ^{ave} is the weighted average temperature, $\theta^{ave} = n\theta^b + (1 - n)\theta^t$, and the item of $\gamma(\theta^{ave} + \tau_1\dot{\theta}^{ave})\delta_{ij}$ in Eq. (7) denotes the thermal effect on the mechanical response; α is the Biot coefficient and $\alpha = 1 - K/K^t$, K, K^t, K^b are the bulk modulus of porous biological tissue, tissue grains and blood; and $1/M = n/K^b + (1 - n)/K^t$, $\gamma^b = K^b a^b$, $\gamma^t = K^b a^b$, $\gamma = Ka^u$, $a^u = na^b + (1 - n)a^t$, a^b, a^t are the linear thermal expansion coefficient of blood and tissue; The last two items on the right-hand side of Eqs. (9) and (10) denote the strain effect on the temperature field; λ and μ are Lamé's constants, ν is Poisson's ratio, and $\lambda = 3K\nu/(1 + \nu)$, $\mu = 3K(1 - 2\nu)/(2(1 + \nu))$; ε_{ij} is the strain tensor and $\varepsilon_{kk} = u_{i,i}$; ξ is the variation of fluid content; δ_{ij} is the Kronecker delta function. τ_1 and τ_2 are the relaxation time factors. It is

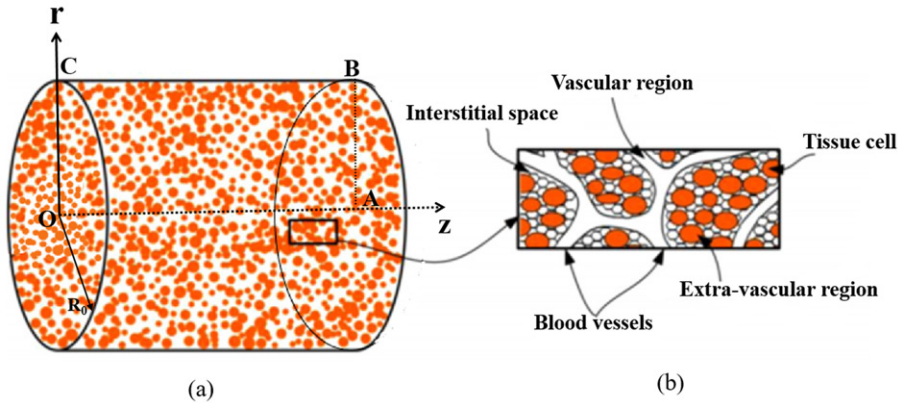


Figure 1. (a) Schematic diagram of the cylindrical biological tissue, (b) porous tissue-vascular structure.

noted that Eqs. (1)–(4), (7)–(10) can be reduced to the LTE model when the temperature of blood and tissue is equal.

f. Geometrical equation

$$\varepsilon_{ij} = \frac{1}{2}(u_{i,j} + u_{j,i}) \tag{11}$$

$$\zeta = w_{i,i} \tag{12}$$

2.2. Problem description

We consider a cylindrical porous biological tissue as shown in Figure 1. The radius of biological tissue is R_0 , the thickness in axis direction is L . In this study, the laser heating is the sole source that directly affects the temperature field and the subsequent mechanical response. When the laser beam such as some UV and IR wavelengths is highly absorbed by the tissue, the laser can be absorbed within a very small depth. In this case, laser heating can be reasonably considered as a surface heat flux on the irradiated boundary [25]. On the contrary, for the cases that scattering phenomenon is significant over the visible and near-infrared wavelengths, laser energy should be served as a spatially varied body heat source to heat up the tissue [26, 27]. An axisymmetric volumetric laser heat source induced by a Gaussian laser beam in space is used in this work [28]:

$$Q^{ext} = \mu_a \phi(r, z, t) \tag{13}$$

$$\phi(r, z, t) = (1 - R)e^{-(\mu_a + \mu_s)z} e^{-(2r^2/r_0^2)} \phi_0 H(t) \tag{14}$$

where μ_a is the absorption coefficient, μ_s is the scattering coefficient; $\phi(r, z, t)$ is the fluence rate. R is reflection coefficient; ϕ_0 is the maximum laser intensity; r_0 is the Gaussian spatial profile of radius which is defined as the character radial distance at the $1/e^2$ location of the laser intensity; $H(t)$ is the Heaviside unit step function.

Due to the geometry of the structure and loading conditions, this is an axisymmetric case and only the region OABC is considered in this work. Thus the considered functions will depend on the space variables r, z , and time t only. The displacement components have, thus, the following form:

$$u_r = u_r(r, z, t), u_z = u_z(r, z, t), w_r = w_r(r, z, t), w_z = w_z(r, z, t) \tag{15}$$

For convenience, Eqs. (7) and (8) are rewritten in terms of the cylindrical coordinate system as follows:

$$\sigma_{rr} = (\lambda + 2\mu) \frac{\partial u_r}{\partial r} + \lambda \left(\frac{u_r}{r} + \frac{\partial u_r}{\partial r} + \frac{\partial u_z}{\partial z} \right) - \gamma \left(\theta^{ave} + \tau_1 \frac{\partial \theta^{ave}}{\partial t} \right) - \alpha p \tag{16}$$

$$\sigma_{zz} = (\lambda + 2\mu) \frac{\partial u_z}{\partial z} + \lambda \left(\frac{u_r}{r} + \frac{\partial u_r}{\partial r} + \frac{\partial u_z}{\partial z} \right) - \gamma \left(\theta^{ave} + \tau_1 \frac{\partial \theta^{ave}}{\partial t} \right) - \alpha p \tag{17}$$

$$\sigma_{zr} = \sigma_{rz} = \mu \left(\frac{\partial u_r}{\partial z} + \frac{\partial u_z}{\partial r} \right) \tag{18}$$

$$p = M \left(a^u \left(\theta^{ave} + \tau_1 \frac{\partial \theta^{ave}}{\partial t} \right) - \alpha \left(\frac{u_r}{r} + \frac{\partial u_r}{\partial r} + \frac{\partial u_z}{\partial z} \right) + \left(\frac{w_r}{r} + \frac{\partial w_r}{\partial r} + \frac{\partial w_z}{\partial z} \right) \right) \tag{19}$$

Substituting Eqs. (1) and (9) into Eq. (3), we can obtain the blood temperature governing equation in the cylindrical coordinate as follows:

$$\begin{aligned} nk^b \left(\frac{\partial^2 \theta^b}{\partial r^2} + \frac{1}{r} \frac{\partial \theta^b}{\partial r} + \frac{\partial^2 \theta^b}{\partial z^2} \right) + nQ^{ext} &= n\rho^b c^b \left(\frac{\partial \theta^b}{\partial t} + \tau_2 \frac{\partial^2 \theta^b}{\partial t^2} \right) \\ + \gamma^t T_0 \left(\frac{\partial^2 u_r}{\partial r \partial t} + \frac{\partial^2 u_z}{\partial z \partial t} + \frac{1}{r} \frac{\partial u_r}{\partial t} \right) + (\gamma^b T_0 + n\rho^b c^b \theta^b) &\left(\frac{\partial^2 w_r}{\partial r \partial t} + \frac{\partial^2 w_z}{\partial z \partial t} + \frac{1}{r} \frac{\partial w_r}{\partial t} \right) \\ + n\rho^b c^b \left(\frac{\partial w_r}{\partial t} \cdot \frac{\partial \theta^b}{\partial r} + \frac{\partial w_z}{\partial t} \cdot \frac{\partial \theta^b}{\partial z} \right) + (ha + \rho^b \varpi^b c^b) &(\theta^b - \theta^t) \end{aligned} \tag{20}$$

Substituting Eqs. (2) and (10) into Eq. (4), the governing equation of tissue temperature can be written as follows:

$$\begin{aligned} (1 - n)k^t \left(\frac{\partial^2 \theta^t}{\partial r^2} + \frac{1}{r} \frac{\partial \theta^t}{\partial r} + \frac{\partial^2 \theta^t}{\partial z^2} \right) + (1 - n)Q^{met} + (1 - n)Q^{ext} \\ = (1 - n)\rho^t c^t \left(\frac{\partial \theta^t}{\partial t} + \tau_2 \frac{\partial^2 \theta^t}{\partial t^2} \right) + \gamma^t T_0 \left(\frac{\partial^2 u_r}{\partial r \partial t} + \frac{\partial^2 u_z}{\partial z \partial t} + \frac{1}{r} \frac{\partial u_r}{\partial t} \right) \\ + \gamma^b T_0 \left(\frac{\partial^2 w_r}{\partial r \partial t} + \frac{\partial^2 w_z}{\partial z \partial t} + \frac{1}{r} \frac{\partial w_r}{\partial t} \right) + (ha + \rho^b \varpi^b c^b) &(\theta^t - \theta^b) \end{aligned} \tag{21}$$

Making use of Eqs. (12) and (19) and Eq. (5), the equation of fluid can be expressed as follows:

$$\begin{aligned} \frac{1}{\kappa} \frac{\partial w_r}{\partial t} + \frac{\rho^b}{n} \frac{\partial^2 w_r}{\partial t^2} + \rho^b \frac{\partial^2 u_r}{\partial t^2} &= M\alpha \left(\frac{\partial^2 u_r}{\partial r^2} + \frac{\partial^2 u_r}{\partial r \partial z} \right) \\ &+ M\alpha \left(\frac{\partial^2 w_r}{\partial r^2} + \frac{\partial^2 w_r}{\partial r \partial z} \right) - Ma^u \left(\frac{\partial \theta^{ave}}{\partial r} + \tau_1 \frac{\partial^2 \theta^{ave}}{\partial r \partial t} \right) \end{aligned} \tag{22}$$

$$\begin{aligned} \frac{1}{\kappa} \frac{\partial w_z}{\partial t} + \frac{\rho^b}{n} \frac{\partial^2 w_z}{\partial t^2} + \rho^b \frac{\partial^2 u_z}{\partial t^2} &= M\alpha \left(\frac{\partial^2 u_z}{\partial z^2} + \frac{\partial^2 u_z}{\partial r \partial z} \right) \\ &+ M\alpha \left(\frac{\partial^2 w_z}{\partial z^2} + \frac{\partial^2 w_z}{\partial r \partial z} \right) - Ma^u \left(\frac{\partial \theta^{ave}}{\partial z} + \tau_1 \frac{\partial^2 \theta^{ave}}{\partial z \partial t} \right) \end{aligned} \tag{23}$$

Further, the substitution of Eqs. (11), (12), (16), (18) and (19) into Eq. (6), the governing equation of motion along the r-axis can be obtained:

$$\begin{aligned} \rho \frac{\partial^2 u_r}{\partial t^2} + \rho^b \frac{\partial^2 w_r}{\partial t^2} &= (\lambda + \mu + \alpha^2 M) \left(\frac{\partial^2 u_r}{\partial r^2} + \frac{\partial^2 u_z}{\partial r \partial z} \right) + \mu \left(\frac{\partial^2 u_r}{\partial r^2} + \frac{\partial^2 u_r}{\partial z^2} \right) \\ &+ \alpha M \left(\frac{\partial^2 w_r}{\partial r^2} + \frac{\partial^2 w_z}{\partial r \partial z} \right) - (\gamma + \alpha a^u M) \left(\frac{\partial \theta^{ave}}{\partial r} + \tau_1 \frac{\partial^2 \theta^{ave}}{\partial r \partial t} \right) \end{aligned} \tag{24}$$

Finally, substituting Eqs. (11), (12), (17)–(19) into Eq. (6), the governing equation of motion along z-axis can be obtained:

$$\begin{aligned} \rho \frac{\partial^2 u_z}{\partial t^2} + \rho^b \frac{\partial^2 w_z}{\partial t^2} &= (\lambda + \mu + \alpha^2 M) \left(\frac{\partial^2 u_z}{\partial z^2} + \frac{\partial^2 u_r}{\partial r \partial z} \right) + \mu \left(\frac{\partial^2 u_r}{\partial r^2} + \frac{\partial^2 u_r}{\partial z^2} \right) \\ &+ \alpha M \left(\frac{\partial^2 w_z}{\partial z^2} + \frac{\partial^2 w_r}{\partial r \partial z} \right) - (\gamma + \alpha a^u M) \left(\frac{\partial \theta^{ave}}{\partial z} + \tau_1 \frac{\partial^2 \theta^{ave}}{\partial z \partial t} \right) \end{aligned} \tag{25}$$

It is noted that the nonlinear coupling terms (the third and fourth terms in the right-hand side of Eq. (20)) are inherent in the blood temperature control equation, which make it more difficult to solve these coupling governing equations using analytical methods directly. Then, the finite-element method is introduced to solve the coupling nonlinear equations in the next section.

The initial conditions of the problem to be considered are

$$\theta^b = \theta^t = 0; u_r = u_z = w_r = w_z = 0 \tag{26}$$

$$\dot{\theta}^b = \dot{\theta}^t = 0; \dot{u}_r = \dot{u}_z = \dot{w}_r = \dot{w}_z = 0 \tag{27}$$

In the analysis, the time period is selected in such a way that the heat wave and elastic wave cannot arrive at the border of the cylindrical biological model. The boundary conditions can be expressed as follows:

$$\begin{aligned} \text{OA} : u_r = w_r = 0, \theta^b = \theta^t = 0 \\ \text{CB} : u_r = u_z = w_r = w_z = 0, \theta^b = \theta^t = 0 \\ \text{OC} : q^b = q^t = 0 \\ \text{AB} : u_r = u_z = w_r = w_z = 0, \theta^b = \theta^t = 0 \end{aligned} \tag{28}$$

which indicate the biological surface is traction free. And comparing to the high-intensity laser, the surface convection can be neglected, thus we assume no energy exchange through the surface of biological tissue.

For simplicity, the following non-dimensional variables are introduced

$$\begin{aligned} (\bar{r}, \bar{z}, \bar{r}_0) &= \frac{1}{l} (r, z, r_0); (\bar{t}, \bar{\tau}_1, \bar{\tau}_2) = \frac{v}{l} (t, \tau_1, \tau_2); \bar{\sigma} = \frac{\sigma}{(\lambda + 2\mu)} \\ (\bar{u}_r, \bar{u}_z, \bar{w}_r, \bar{w}_z) &= \frac{1}{l} (u_r, u_z, w_r, w_z); (\bar{\theta}^b, \bar{\theta}^t, \bar{\theta}^{ave}) = \frac{1}{T_0} (\theta^b, \theta^t, \theta^{ave}) \\ \bar{p} &= \frac{\alpha p}{(\lambda + 2\mu)}; (\bar{Q}^{met}, \bar{Q}^{ext}) = \frac{l^2}{kT_0} (Q^{met}, Q^{ext}); v = \sqrt{(\lambda + 2\mu)/\rho^t} \end{aligned}$$

where l and v are the characteristic length and velocity, respectively. The short lines over the non-dimensional variables are dropped in the following for the sake of brevity.

2.3. Finite element formulation

The presence of nonlinear governing equation of blood temperature field causes the difficulty in solving the problem. It is noted that the nonlinear coupled terms are inherently in the governing equations of generalized thermoelasticity problems in the context of the LTNE model. The nonlinear governing equations in the Laplace/Fourier transformation domain are also difficult to be solved. Even if the solutions are obtained, the discrete error and truncate error are inevitably introduced in the numerical inverse process [29, 30]. To minimize the errors, finite-element method in time-domain is used in this work for solving coupled nonlinear thermomechanical equations [31]. In order to obtain the finite-element governing equations conveniently, Eqs. (7)–(10) can be written in matrix forms:

$$\begin{aligned} \{\sigma\} &= [C_0]\{\varepsilon\} - \{n(\gamma + a^u \alpha M)\}(\theta^b + \tau_1 \dot{\theta}^b) \\ &\quad - \{(1 - n)(\gamma + a^u \alpha M)\}(\theta^t + \tau_1 \dot{\theta}^t) - [\alpha M]\{\xi\} \end{aligned} \tag{29}$$

$$\{p\} = [M]\{\xi\} - [\alpha M]^T \{\varepsilon\} + [na^u M](\theta^b + \tau_1 \dot{\theta}^b) + [(1 - n)a^u M](\theta^t + \tau_1 \dot{\theta}^t) \tag{30}$$

$$\rho^b S^b = \{\gamma^t\}^T \{\varepsilon\} + \{\gamma^b\}^T \{\xi\} + c_1(\theta^b + \tau_2 \dot{\theta}^b) \tag{31}$$

$$\rho^t S^t = \{\gamma^t\}^T \{\varepsilon\} + \{\gamma^b\}^T \{\xi\} + c_2(\theta^t + \tau_2 \dot{\theta}^t) \tag{32}$$

where $c_1 = n\rho^b c^b / T_0$, $c_2 = (1 - n)\rho^t c^t / T_0$.

The basic constitutive variables are temperature and displacement of tissue and blood. According to the finite-element method, the geometrical domain can be subdivided into a finite number of regions or elements. In each element, the displacement and temperature can be expressed as four sets of shape functions:

$$\{u\} = [N_1]\{u_e\}, \{w\} = [N_2]\{w_e\}, \{\theta^b\} = [N_3]\{\theta_e^b\}, \{\theta^t\} = [N_4]\{\theta_e^t\} \tag{33}$$

The strain and temperature gradient may be expressed as follows:

$$\{\varepsilon\} = [B_1]\{u_e\}, \{\xi\} = [B_2]\{w_e\}, \{\hat{\theta}^b\} = [B_3]\{\theta_e^b\}, \{\hat{\theta}^t\} = [B_4]\{\theta_e^t\} \tag{34}$$

where e is the number of elements; $[N_1]$, $[N_2]$, $[N_3]$ and $[N_4]$ are the shape functions; $[B_1]$, $[B_2]$, $[B_3]$ and $[B_4]$ are derived from $[N_1]$, $[N_2]$, $[N_3]$ and $[N_4]$, respectively; and $\hat{\theta}^b = \theta_{,p}^b$, $\hat{\theta}^t = \theta_{,i}^t$. The principle of virtual displacement for the generalized thermo-elasticity yields,

$$\begin{aligned} &\int_V \left[\delta\{\varepsilon\}^T \{\sigma\} + \delta\{\hat{\theta}^b\}^T \{q^b\} + \delta\{\hat{\theta}^t\}^T \{q^t\} + \delta\{\xi\}^T \{p\} \right] dV \\ &\quad - \delta\{\theta^b\} \rho^b T_0 \{\dot{S}^b\} - \delta\{\theta^t\} \rho^t T_0 \{\dot{S}^t\} \\ &= - \int_V \delta\{u\}^T \rho \{\ddot{u}\} dV - \int_V \delta\{w\}^T \rho^b \{\ddot{w}\} dV + \int_{A_\sigma} \delta\{u\}^T \{\tilde{T}_1\} dA \\ &\quad + \int_{A_p} \delta\{w\}^T \{\tilde{T}_2\} dA + \int_{A_q^b} \delta\theta^b \tilde{q}^b dA + \int_{A_q^t} \delta\theta^t \tilde{q}^t dA \end{aligned} \tag{35}$$

where $\{\tilde{T}_1\}$, $\{\tilde{T}_2\}$ and \tilde{q}^b, \tilde{q}^t represent the traction and heat flux acted on surface A_σ, A_p, A_q^b , and A_q^t , respectively. And

$$\begin{aligned} \int_V \delta\{\varepsilon\}^T \{\sigma\} dV &= \delta\{u_e\}^T \int_V [B_1]^T ([C_0][B_1]\{u_e\} - [\alpha M][B_2]\{w_e\}) dV \\ &\quad - \delta\{u_e\}^T \int_V [B_1]^T \{n(\gamma + a^u \alpha M)\} [N_3]\{\theta_e^b + \tau_1 \dot{\theta}_e^b\} dV \\ &\quad - \delta\{u_e\}^T \int_V [B_1]^T \{(1 - n)(\gamma + a^u \alpha M)\} [N_4]\{\theta_e^t + \tau_1 \dot{\theta}_e^t\} dV \end{aligned} \tag{36}$$

$$\begin{aligned} \int_V \delta\{\hat{\theta}^b\}^T \{q^b\} dV &= -\delta\{\theta_e^b\}^T nk^b \int_V [B_3]^T [B_3]\{\theta_e^b\} dV \\ &\quad + \delta\{\theta_e^b\}^T n\rho^b c^b \int_V [B_3]^T [N_3][N_2]\{\theta_e^b\} \{\dot{w}_e\} dV \end{aligned} \tag{37}$$

$$\int_V \delta\{\hat{\theta}^t\}^T \{q^t\} dV = -\delta\{\theta_e^t\}^T (1 - n)k^t \int_V [B_4]^T [B_4]\{\theta_e^t\} dV \tag{38}$$

$$\int_V \delta\{\xi\}^T \{p\} dV = \delta\{w_e\}^T \int_V [B_2]^T ([M][B_2]\{w_e\} - [\alpha M]^T [B_1]\{u_e\}) dV + \delta\{w_e\}^T \int_V [B_2]^T [na^u M][N_3](\{\theta_e^b\} + \tau_1 \{\dot{\theta}_e^b\}) dV + \delta\{w_e\}^T \int_V [B_2]^T [(1-n)a^u M][N_4](\{\theta_e^t\} + \tau_1 \{\dot{\theta}_e^t\}) dV \tag{39}$$

$$\int_V \delta\{\theta^b\} \rho^b T_0 \{\dot{S}^b\} dV = \delta\{\theta_e^b\} T_0 \int_V [N_3] \{\gamma^t\}^T [B_1] \{\dot{u}_e\} dV + \delta\{\theta_e^b\} T_0 \int_V [N_3] \left(\{\gamma^b\}^T [B_2] \{\dot{w}_e\} + c_1 [N_3] (\{\dot{\theta}_e^b\} + \tau_2 \{\ddot{\theta}_e^b\}) \right) dV \tag{40}$$

$$\int_V \delta\{\theta^t\} \rho^t T_0 \{\dot{S}^t\} dV = \delta\{\theta_e^t\} T_0 \int_V [N_4] \{\gamma^t\}^T [B_1] \{\dot{u}_e\} dV + \delta\{\theta_e^t\} T_0 \int_V [N_4] \left(\{\gamma^b\}^T [B_2] \{\dot{w}_e\} + c_2 [N_4] (\{\dot{\theta}_e^t\} + \tau_2 \{\ddot{\theta}_e^t\}) \right) dV \tag{41}$$

$$\int_V \delta\{u\}^T \rho \{\ddot{u}\} dV = \delta\{u_e\}^T \int_V [N_1]^T [N_1] \{\ddot{u}_e\} dV \tag{42}$$

$$\int_V \delta\{w\}^T \rho^b \{\ddot{w}\} dV = \delta\{w_e\}^T \rho^b \int_V [N_2]^T [N_2] \{\ddot{w}_e\} dV \tag{43}$$

$$\int_{A_\sigma} \delta\{u\}^T \{\tilde{T}_1\} dA = \delta\{u_e\}^T \int_{A_\sigma} [N_1]^T \{\tilde{T}_1\} dA = \delta\{u_e\}^T \{F_e^m\} \tag{44}$$

$$\int_{A_p} \delta\{w\}^T \{\tilde{T}_2\} dA = \delta\{w_e\}^T \int_{A_p} [N_2]^T \{\tilde{T}_2\} dA = \delta\{u_e\}^T \{F_e^f\} \tag{45}$$

$$\int_{A_q^b} \delta\theta^b \tilde{q}^b dA = \delta\{\theta_e^b\} \int_{A_q^b} [N_3] \tilde{q}^b dA = \delta\{\theta_e^b\} \{F_e^b\} \tag{46}$$

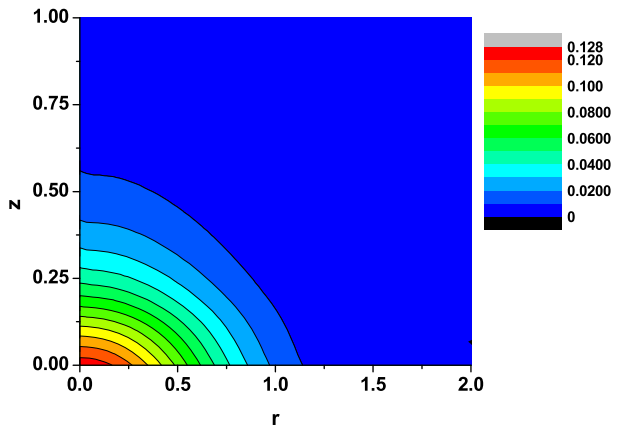
$$\int_{A_q^t} \delta\theta^t \tilde{q}^t dA = \delta\{\theta_e^t\} \int_{A_q^t} [N_4] \tilde{q}^t dA = \delta\{\theta_e^t\} \{F_e^t\} \tag{47}$$

Substituting Eqs. (36)–(47) into Eq. (35), we can obtain the finite-element governing equations as follows:

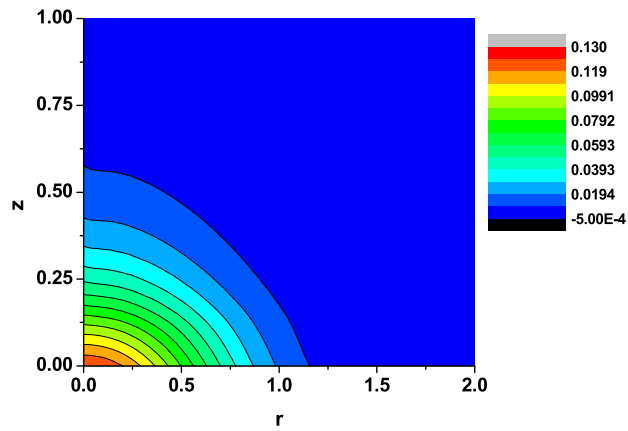
$$\begin{bmatrix} D_e^{11} & 0 & 0 & 0 \\ 0 & D_e^{22} & 0 & 0 \\ 0 & 0 & D_e^{33} & 0 \\ 0 & 0 & 0 & D_e^{44} \end{bmatrix} \begin{bmatrix} \ddot{u}_e \\ \ddot{w}_e \\ \ddot{\theta}_e^b \\ \ddot{\theta}_e^t \end{bmatrix} + \begin{bmatrix} 0 & 0 & C_e^{13} & C_e^{14} \\ 0 & 0 & C_e^{23} & C_e^{24} \\ C_e^{31} & C_e^{32} & C_e^{33} & 0 \\ C_e^{41} & C_e^{42} & 0 & C_e^{44} \end{bmatrix} \begin{bmatrix} \dot{u}_e \\ \dot{w}_e \\ \dot{\theta}_e^b \\ \dot{\theta}_e^t \end{bmatrix} + \begin{bmatrix} K_e^{11} & -K_e^{12} & -K_e^{13} & -K_e^{14} \\ -K_e^{21} & K_e^{22} & K_e^{23} & K_e^{24} \\ 0 & 0 & K_e^{33} & 0 \\ 0 & 0 & 0 & K_e^{44} \end{bmatrix} \begin{bmatrix} u_e \\ w_e \\ \theta_e^b \\ \theta_e^t \end{bmatrix} = \begin{bmatrix} F_e^m \\ F_e^f \\ F_e^b \\ F_e^t \end{bmatrix} \tag{48}$$

Table 1. The material parameters of biological tissue.

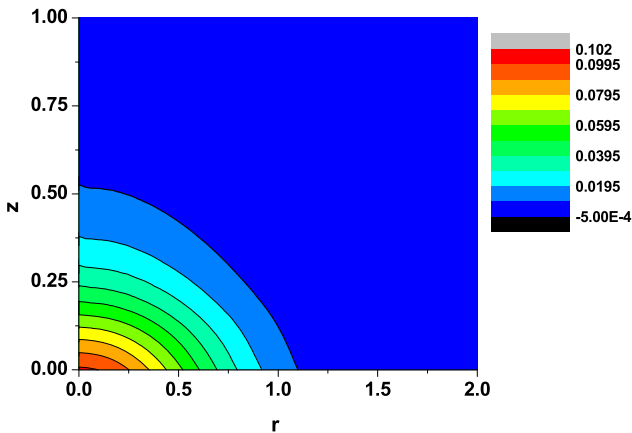
$K = 6.87 \times 10^6 \text{pa}$	$K^t = 7.4 \times 10^7 \text{pa}$	$K^b = 1.0 \times 10^9 \text{pa}$	$\nu = 0.48$
$\rho^t = 1000 \text{kg/m}^3$	$\rho^b = 1060 \text{kg/m}^3$	$k^t = 0.4 \text{W/m/K}$	$k^b = 0.5 \text{W/m/K}$
$c^t = 4200 \text{J/kg/K}$	$c^b = 3900 \text{J/kg/K}$	$a^t = 10^{-4} / \text{K}$	$a^b = 10^{-4} / \text{K}$
$k^t = 10^{-4} \text{m/s}$	$T_0 = 310 \text{K}$	$\mu_a = 120 \text{m}^{-1}$	$\mu_s = 1700 \text{m}^{-1}$
$\varpi^b = 0.005 \text{s}^{-1}$	$Q^{met} = 380 \text{W/m}^3$	$\phi_0 = 1.6 \times 10^5 \text{W/m}^2$	$R = 0.4$
$ha = 53592 \text{W/m}^2 \text{K}$			



(a) Tissue temperature in LNTE model



(b) Blood temperature in LNTE model



(c) Temperature in LTE model

Figure 2. Temperature contours in the LNTE and LTE models. (a) Tissue temperature in the LNTE model, (b) Blood temperature in the LNTE model, and (c) Temperature in the LTE model.

where $[D]$, $[C]$ and $[K]$ are the mass, damping and stiffness matrices, respectively. $\{F_e^m F_e^f F_e^b F_e^t\}^T$ are the load vectors associated with the boundary conditions. The coefficients and load vectors in Eq. (48) are

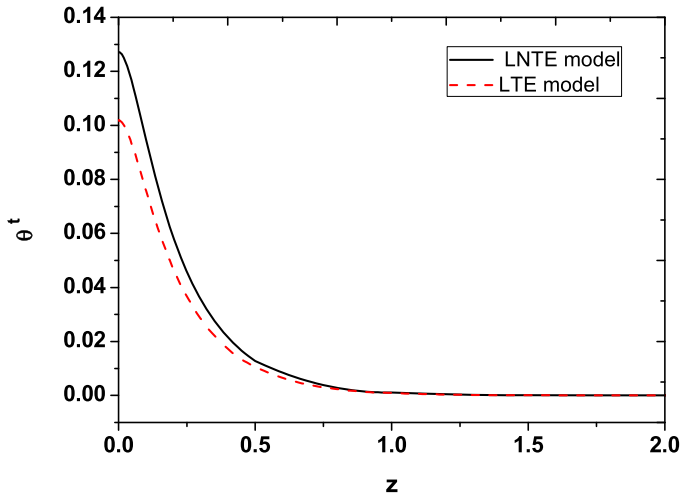


Figure 3. The distribution of tissue temperature along OA.

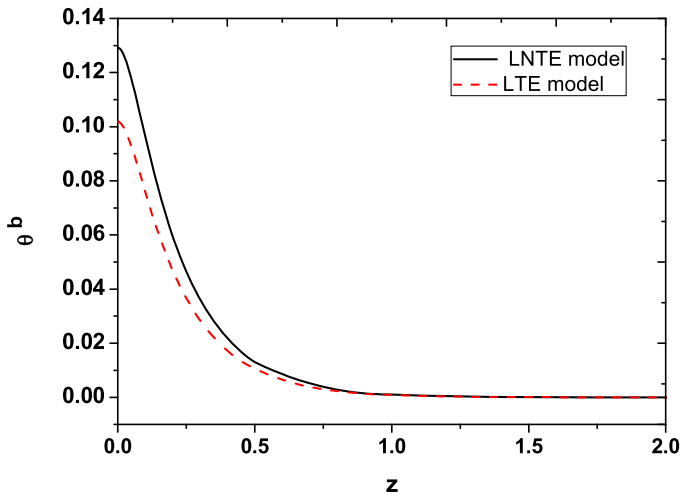


Figure 4. The distribution of blood temperature along OA.

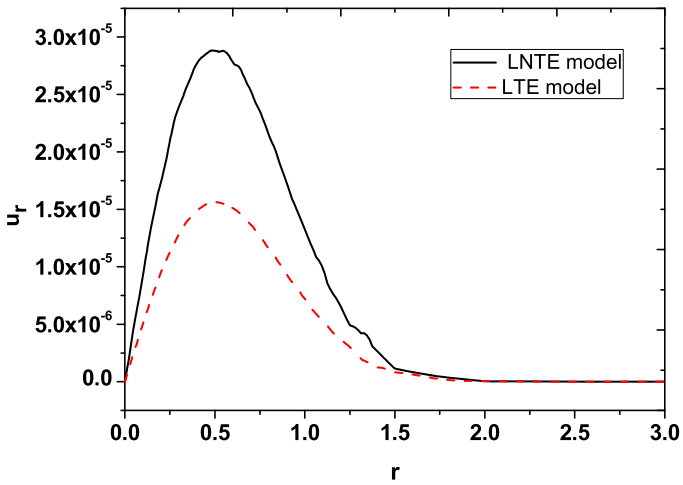


Figure 5. The distribution of displacement u_r along OC.

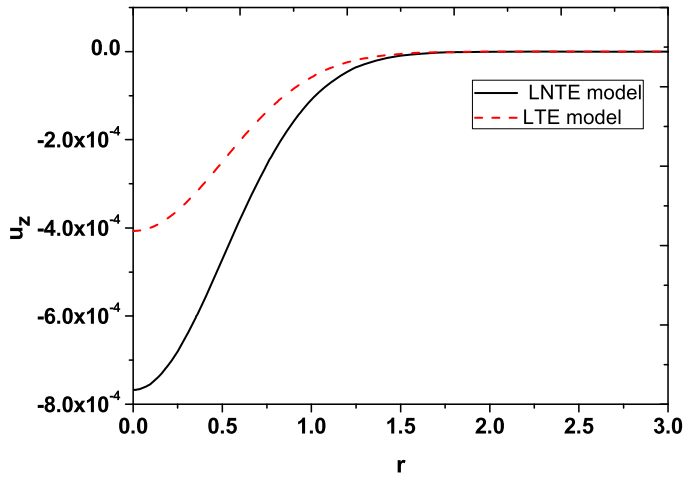


Figure 6. The distribution of displacement u_z along OC.

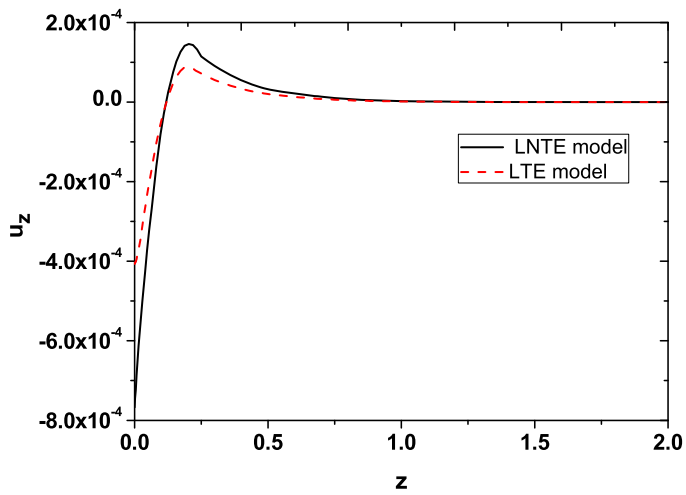


Figure 7. The distribution of displacement u_z along OA.

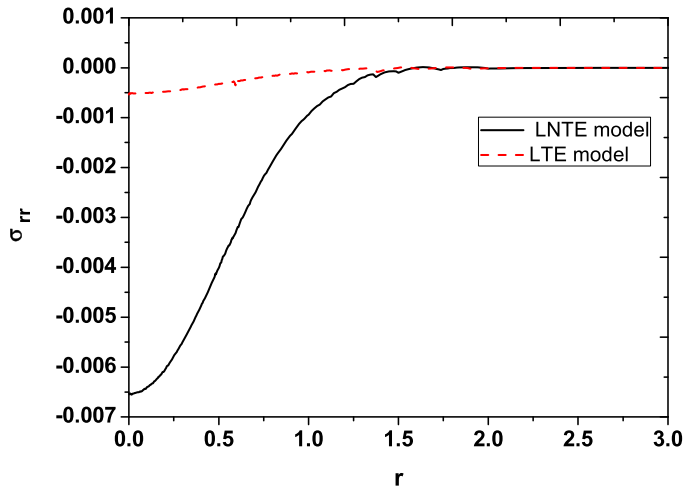


Figure 8. The distribution of stress σ_{rr} along OC.

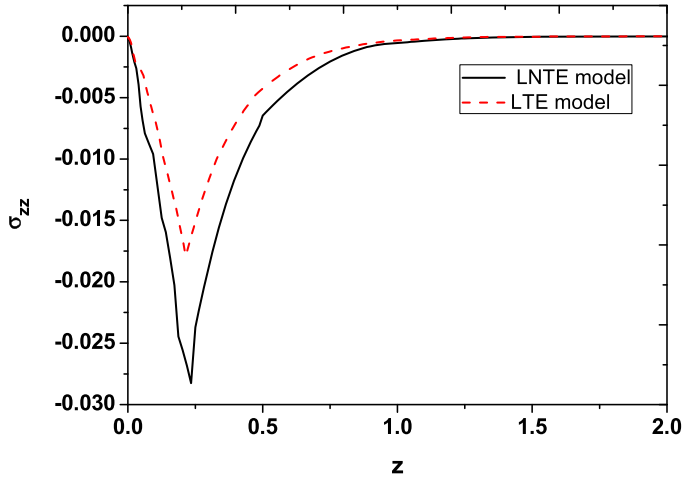


Figure 9. The distribution of stress σ_{zz} along OA.

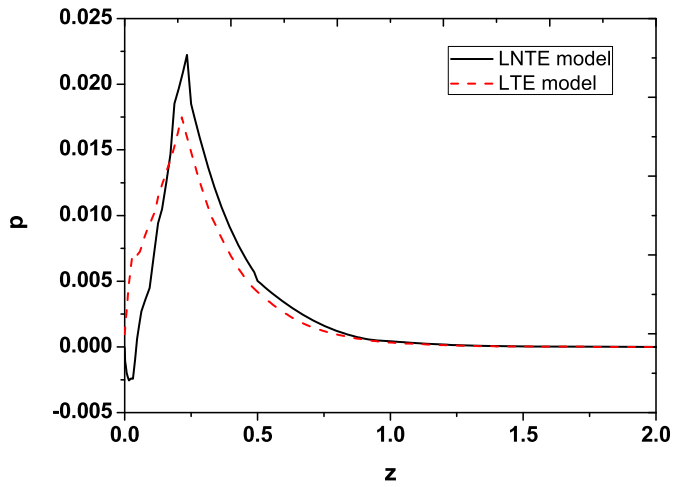


Figure 10. The distribution of pressure p along OA.

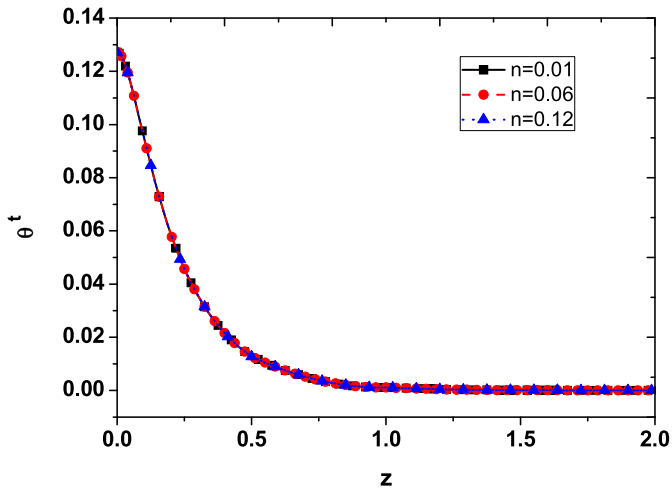


Figure 11. The effect of porosity coefficient on tissue temperature along OA.

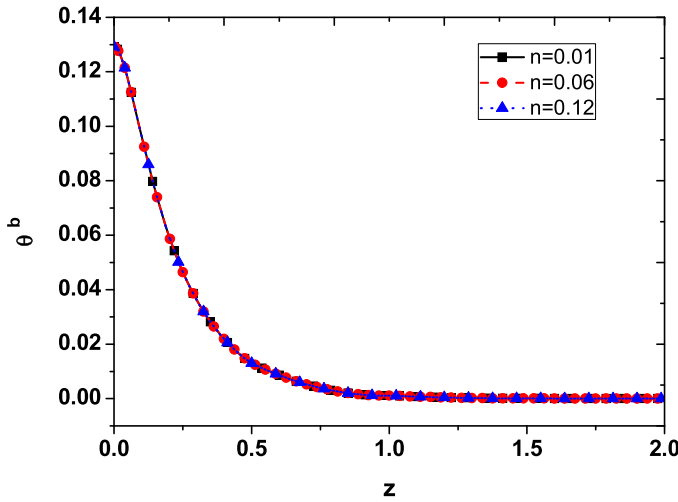


Figure 12. The effect of porosity coefficient on blood temperature along OA.

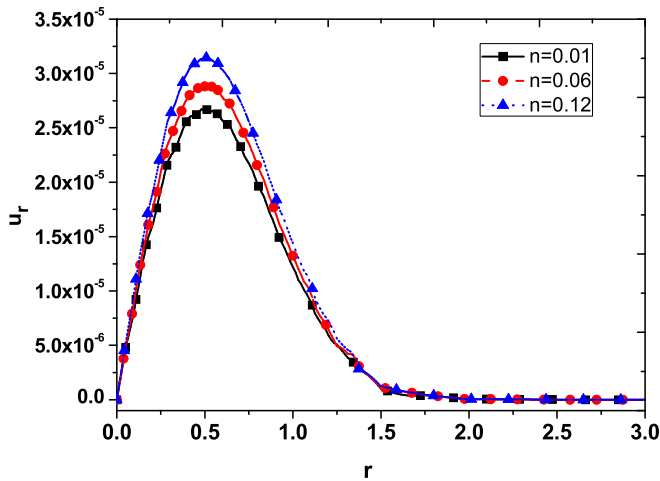


Figure 13. The effect of porosity coefficient on radial displacement along OC.

given in the appendix. It should be emphasized that the matrix $[C_e^{32}]$ is nonlinear, which is different from that in [32]. Thus far, finite-element formulations of generalized thermo-mechanical problem base on the LTNE model are obtained. Then, the finite-element equations (Eq. (48)) can be solved directly using the software Flexpde in time domain with the initial and boundary conditions.

2.4. Numerical results and discussions

In the calculation, the material parameters of biological tissue are shown in Table 1 [16, 28, 33]. The non-dimensional lengths are $OA = OC = 5.0$, $r_0 = 1.0$, respectively. The non-dimensional time $t = 0.12$, $\tau_1 = \tau_2 = 0.04$ are used in the following numerical example.

To investigate the effects of local thermal non-equilibrium model on the thermal-mechanical response in porous biological tissue when the porosity coefficient is 0.06, the results of the LTE model are also given. Figure 2 show the temperature contours in the context of LNTE and LTE models. It can be found that the temperature changed zone is in a finite area. The changed zone of the LNTE model is larger than the LTE model. Outside this region, the temperature is almost unchanged.

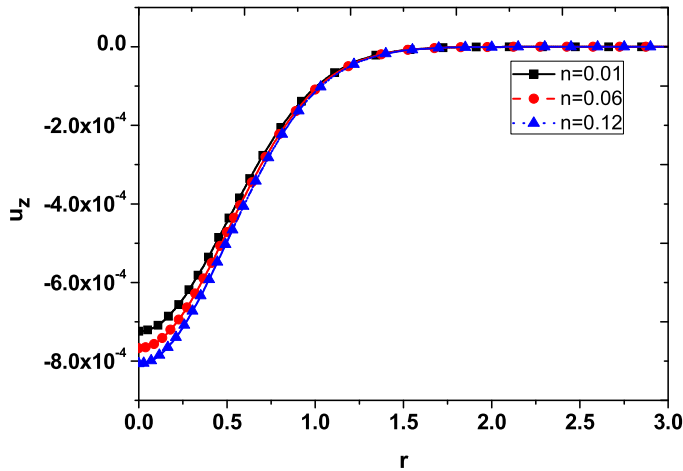


Figure 14. The effect of porosity coefficient on axial displacement along OC.

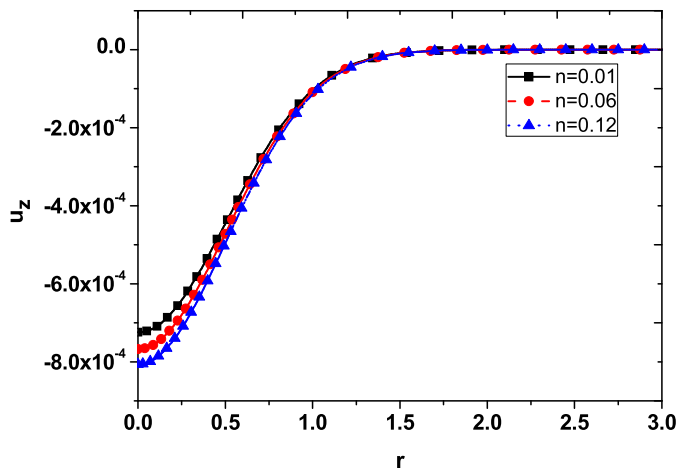


Figure 15. The effect of porosity coefficient on axial displacement along OA.

To further study, the discrepancies of these two models on the transient responses, the results along OA and OC are pictured in Figures 3–10. In Figures 3 and 4, it can be seen that the temperature at the origin predicted by LNTE model are larger than the LTE model when subject to the same external energy. This phenomenon may be caused by the thermal effects of blood perfusion and convective in the LNTE model. Figure 5 shows the distribution of radial displacement along OC. The radial displacement of the origin is zero. This is consistent with the axial symmetry condition. The distributions of axial displacement along OC and OA are plotted in Figures 6 and 7, respectively. The axial displacement u_z along OC is always negative. This indicates that the surface of biological tissue suffers thermal expansion deformation and moves to the unconstrained direction. It can be seen from Figure 7 that the axial displacement at the origin is the largest and the direction is opposite to the z -axis. From Figure 8, we can see that the stress σ_{rr} is always negative and approaches to zero along OC. The stress σ_{zz} at the origin is zero (traction-free surface) and increases as moving away from the origin in Figure 9. The zero excess pore pressure on the origin is consisted with the boundary condition in Figure 10.

The effects of porosity coefficient on the responses in the context of the LNTE model are shown in Figures 11–18. Form Figures 11 and 12, we can see the porosity coefficient has little

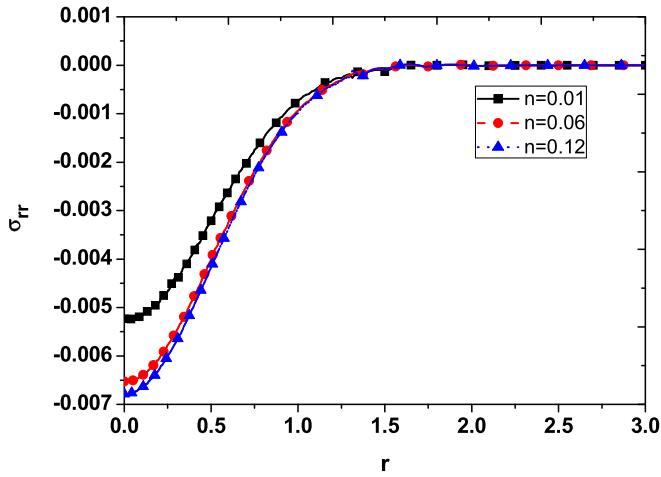


Figure 16. The effect of porosity coefficient on radial stress along OC.

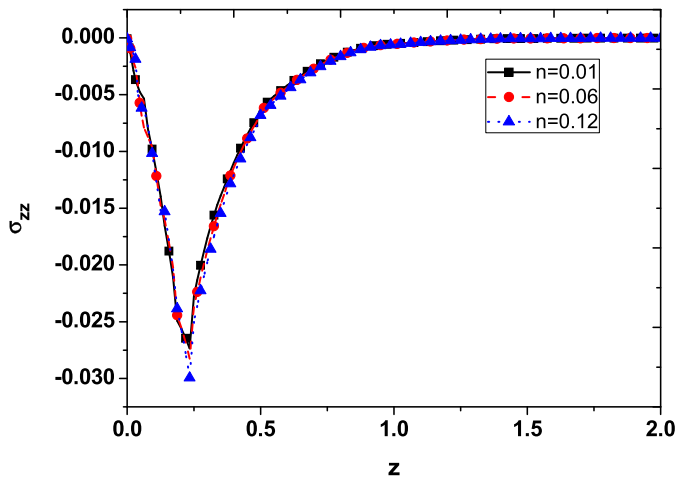


Figure 17. The effect of porosity coefficient on axial stress along OA.

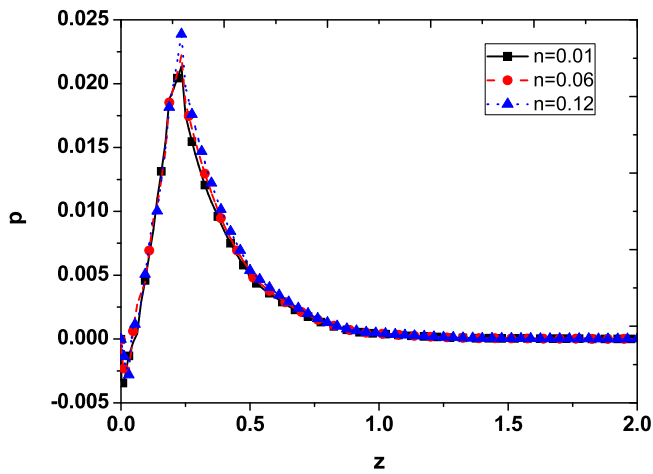


Figure 18. The effect of porosity coefficient on pressure along OA.

effect on tissue and blood temperature. This thermal conductivity of tissue is very close to thermal conductivity of blood. It can be seen that porosity coefficient n has a significant effect on the displacement, stress and excess pore pressure in Figures 13–18. The maximum absolute values of displacement, stress and excess pore pressure increase with the increase of porosity coefficient.

3. Conclusions

The presence of blood and its thermal roles in living tissue such as blood perfusion and convection, make it is quite natural to treat the living tissue as a porous medium. Based on a non-equilibrium heat transfer model, we investigate the transient coupled thermomechanical response of porous biological tissue in the context of generalized thermoelastic theory. The nonlinear finite-element governing equations are established and solved in time-domain. Comparisons are presented with LTNE and LTE models to investigate the difference of these two models on the thermoelastic response. From the numerical results, one may conclude that the temperature, displacement and stress of the LNTE model are larger than the LTE model. The magnitudes of displacement, stress and excess pore pressure increase with the increasing of porosity coefficient n . The porosity coefficient has little influence on temperature change.

Appendix

The coefficients and load vectors in Eq. (48) are listed below:

$$\begin{aligned}
 [D_e^{11}] &= \int_V [N_1]^T \rho [N_1] dV, [D_e^{22}] = \int_V [N_2]^T \rho^b [N_2] dV, \\
 [D_e^{33}] &= T_0 c_1 \tau_2 \int_V [N_3] [N_3] dV, [D_e^{44}] = T_0 c_2 \tau_2 \int_V [N_4] [N_4] dV, \\
 [C_e^{13}] &= \int_V n \tau_1 [B_1]^T [\gamma + a^\mu \alpha M] [N_3]^T dV, [C_e^{14}] = \int_V (1-n) \tau_1 [B_1]^T [\gamma + a^\mu \alpha M] [N_4]^T dV, \\
 [C_e^{23}] &= \int_V [B_2]^T [n \tau_1 a^\mu M] [N_3] dV, [C_e^{24}] = \int_V [B_2]^T [(1-n) \tau_1 a^\mu M] [N_4] dV, \\
 [C_e^{31}] &= T_0 \int_V \{\gamma_t\}^T [B_1] [N_3] dV, [C_e^{33}] = T_0 c_1 \int_V [N_3] [N_3] dV, \\
 [C_e^{32}] &= T_0 \int_V (\{\gamma^b\}^T [B_2] [N_3] + n \rho^b c^b [B_3]^T [N_3] [N_2] \{\theta_e^b\}) dV, \\
 [C_e^{41}] &= T_0 \int_V \{\gamma^t\}^T [B_1] [N_4] dV, [C_e^{42}] = T_0 \int_V \{\gamma^b\}^T [B_2] [N_4] dV, \\
 [C_e^{44}] &= T_0 c_2 \int_V [N_4] [N_4] dV, [K_e^{11}] = \int_V [B_1]^T [C_0] [B_1] dV, \\
 [K_e^{12}] &= \int_V [B_1]^T [\alpha M] [B_2] dV, [K_e^{13}] = \int_V [B_1]^T n [\gamma + a^\mu \alpha M] [N_3]^T dV, \\
 [K_e^{14}] &= \int_V [B_1]^T (1-n) [\gamma + a^\mu \alpha M] [N_4]^T dV, [K_e^{21}] = \int_V [B_2]^T [\alpha M]^T [B_1] dV, \\
 [K_e^{22}] &= \int_V [B_2]^T [\alpha M] [B_2] dV, [K_e^{23}] = \int_V [B_2]^T [n a^\mu M] [N_3] dV, \\
 [K_e^{24}] &= \int_V [B_2]^T [(1-n) a^\mu M] [N_4] dV, [K_e^{33}] = -n k^b \int_V [B_3]^T [B_3] dV, \\
 [K_e^{44}] &= -(1-n) k^t \int_V [B_4]^T [B_4] dV, \{F_e^m\} = \int_{A_\sigma} [N_1]^T \{\bar{T}\} dA, \{F_e^f\} = \int_{A_p} [N_2]^T \{\bar{T}\} dA, \\
 \{F_e^b\} &= - \int_{A_q^b} [N_3]^T \{\bar{q}^b\} dA, \{F_e^t\} = - \int_{A_q^t} [N_4]^T \{\bar{q}^t\} dA
 \end{aligned}$$

Funding

This work was supported by the National Science Foundation of China (11732007, 11572237), the Fundamental Research Funds for the Central Universities and the State Scholarship Fund from the China Scholarship Council (CSC).

References

- [1] B. Alazmi and K. Vafai, "Analysis of variants within the porous media transport models," *ASME J. Heat Transfer*, vol. 122, no. 2, pp. 303–326, 1999. DOI: [10.1115/1.521468](https://doi.org/10.1115/1.521468).
- [2] H. S. Kou, T. C. Shih, and W. L. Lin, "Effect of the directional blood flow on thermal dose distribution during thermal therapy: An application of a Green's function based on the porous model," *Phys. Med. Biol.*, vol. 48, no. 11, pp. 1577–1589, 2003. DOI: [10.1088/0031-9155/48/11/307](https://doi.org/10.1088/0031-9155/48/11/307).
- [3] P. Rattanadecho and P. Keangin, "Numerical study of heat transfer and blood flow in two-layered porous liver tissue during microwave ablation process using single and double slot antenna," *Int. J. Heat Mass Transfer*, vol. 58, no. 1/2, pp. 457–470, 2013. no DOI: [10.1016/j.ijheatmasstransfer.2012.10.043](https://doi.org/10.1016/j.ijheatmasstransfer.2012.10.043).
- [4] L. Cao, Q. H. Qin, and N. Zhao, "An RBF-MFS model for analysing thermal behaviour of skin tissues," *Int. J. Heat Mass Transfer*, vol. 53, no. 7/8, pp. 1298–1307, 2010. no DOI: [10.1016/j.ijheatmasstransfer.2009.12.036](https://doi.org/10.1016/j.ijheatmasstransfer.2009.12.036).
- [5] P. Yuan, "Numerical analysis of temperature and thermal dose response of biological tissues to thermal non-equilibrium during hyperthermia therapy," *Med. Eng. Phys.*, vol. 30, no. 2, pp. 135–143, 2008. DOI: [10.1016/j.medengphy.2007.03.006](https://doi.org/10.1016/j.medengphy.2007.03.006).
- [6] A. R. A. Khaled and K. Vafai, "The role of porous media in modeling flow and heat transfer in biological tissues," *Int. J. Heat Mass Transfer*, vol. 46, no. 26, pp. 4989–5003, 2003. DOI: [10.1016/S0017-9310\(03\)00301-6](https://doi.org/10.1016/S0017-9310(03)00301-6).
- [7] Y. Zhang, "Generalized dual-phase lag bioheat equations based on nonequilibrium heat transfer in living biological tissues," *Int. J. Heat Mass Transfer*, vol. 52, no. 21-22, pp. 4829–4834, 2009. DOI: [10.1016/j.ijheatmasstransfer.2009.06.007](https://doi.org/10.1016/j.ijheatmasstransfer.2009.06.007).
- [8] J. Fan and L. Wang, "A general bioheat model at macroscale," *Int. J. Heat Mass Transfer*, vol. 54, no. 1–3, pp. 722–726, 2011. DOI: [10.1016/j.ijheatmasstransfer.2010.09.052](https://doi.org/10.1016/j.ijheatmasstransfer.2010.09.052).
- [9] N. Afrin, Y. Zhang, and J. K. Chen, "Thermal lagging in living biological tissue based on nonequilibrium heat transfer between tissue, arterial and venous bloods," *Int. J. Heat Mass Transfer*, vol. 54, no. 11/12, pp. 2419–2426, 2011. DOI: [10.1016/j.ijheatmasstransfer.2011.02.020](https://doi.org/10.1016/j.ijheatmasstransfer.2011.02.020).
- [10] Y. M. Xuan and W. Roetzel, "Bioheat equation of the human thermal system," *Chem. Eng. Technol.*, vol. 20, no. 4, pp. 268–276, 1997. DOI: [10.1002/ceat.270200407](https://doi.org/10.1002/ceat.270200407).
- [11] Y. M. Xuan and W. Roetzel, "Transfer response of the human limb to an external stimulus," *Int. J. Heat Mass Transfer*, vol. 41, pp. 229–239, 1998. DOI: [10.1016/S0017-9310\(96\)00160-3](https://doi.org/10.1016/S0017-9310(96)00160-3).
- [12] S. Mahjoob and K. Vafai, "Analytical characterization of heat transport through biological media incorporating hyperthermia treatment," *Int. J. Heat Mass Transfer*, vol. 52, no. 5/6, pp. 1608–1618, 2009. DOI: [10.1016/j.ijheatmasstransfer.2008.07.038](https://doi.org/10.1016/j.ijheatmasstransfer.2008.07.038).
- [13] P. Yuan, "Numerical analysis of an equivalent heat transfer coefficient in a porous model for simulating a biological tissue in a hyperthermia therapy," *Int. J. Heat Mass Transfer*, vol. 52, no. 7-8, pp. 1734–1740, 2009. DOI: [10.1016/j.ijheatmasstransfer.2008.09.033](https://doi.org/10.1016/j.ijheatmasstransfer.2008.09.033).
- [14] A. Belmiloudi, "Parameter identification problems and analysis of the impact of porous media in biofluid heat transfer in biological tissues during thermal therapy," *Nonlinear Anal.: Real World Appl.*, vol. 11, no. 3, pp. 1345–1363, 2010. DOI: [10.1016/j.nonrwa.2009.02.025](https://doi.org/10.1016/j.nonrwa.2009.02.025).
- [15] C. P. Lau, Y. T. Tai, and P. W. Lee, "The effects of radio frequency ablation versus medical therapy on the quality-of-life and exercise capacity in patients with accessory pathway-mediated supraventricular tachycardia: A treatment comparison study," *Pacing Clin. Electro.*, vol. 18, no. 3, pp. 424–432, 1995. DOI: [10.1111/j.1540-8159.1995.tb02541.x](https://doi.org/10.1111/j.1540-8159.1995.tb02541.x).
- [16] P. Keangin, T. Wessapan, and P. Rattanadecho, "Analysis of heat transfer in deformed liver cancer modeling treated using a microwave coaxial antenna," *Appl. Therm. Eng.*, vol. 31, no. 16, pp. 3243–3254, 2011. DOI: [10.1016/j.applthermaleng.2011.06.005](https://doi.org/10.1016/j.applthermaleng.2011.06.005).
- [17] X. Y. Li, C. L. Li, Z. N. Xue, and X. G. Tian, "Analytical study of transient thermo-mechanical responses of dual-layer skin tissue with variable thermal material properties," *Int. J. Thermal Sci.*, vol. 124, pp. 459–466, 2018. DOI: [10.1016/j.ijthermalsci.2017.11.002](https://doi.org/10.1016/j.ijthermalsci.2017.11.002).
- [18] X. Yang, "Gurtin-type variational principles for dynamics of a non-local thermal equilibrium saturated porous medium," *Acta Mech. Solida Sin.*, vol. 18, pp. 37–45, 2005.
- [19] L. W. He and X. Yang, "Quasi-static and dynamic behavior of incompressible saturated poroelastic one-dimensional column on local thermal nonequilibrium," *J. Mech. MEMS*, vol. 1, pp. 289–299, 2009.

- [20] L. W. He and Z. H. Jin, "A local thermal nonequilibrium poroelastic theory for fluid saturated porous media," *J. Therm. Stresses*, vol. 33, no. 8, pp. 799–813, 2010. DOI: [10.1080/01495739.2010.482358](https://doi.org/10.1080/01495739.2010.482358).
- [21] L. W. He, Z. H. Jin, and Y. Zhang, "Convective cooling/heating induced thermal stresses in a fluid saturated porous medium undergoing local thermal non-equilibrium," *Int. J. Solids Struct.*, vol. 49, no. 5, pp. 748–758, 2012. DOI: [10.1016/j.ijsolstr.2011.11.014](https://doi.org/10.1016/j.ijsolstr.2011.11.014).
- [22] H. W. Lord and Y. Shulman, "A generalized dynamical theory of thermoelasticity," *J. Mech. Phys. Solids*, vol. 15, no. 5, pp. 299–309, 1967. DOI: [10.1016/0022-5096\(67\)90024-5](https://doi.org/10.1016/0022-5096(67)90024-5).
- [23] A. E. Green and K. A. Lindsay, "Thermoelasticity," *J. Elasticity*, vol. 2, no. 1, pp. 1–7, 1972. DOI: [10.1007/BF00045689](https://doi.org/10.1007/BF00045689).
- [24] E. Detournay, and A. H. D. Cheng, "Fundamentals of poroelasticity," in *Comprehensive Rock Engineering: Principles, Practice and Projects. Vol. II, Analysis and Design Method*. C. Fairhurst, Ed. Oxford, Pergamon Press, 1993, pp. 113–171.
- [25] K. Wang, F. Tavakkoli, S. Wang *et al.*, "Analysis and analytical characterization of bioheat transfer during radiofrequency ablation," *J. Biomech.*, vol. 48, no. 6, pp. 930–940, 2015. DOI: [10.1016/j.jbiomech.2015.02.023](https://doi.org/10.1016/j.jbiomech.2015.02.023).
- [26] A. J. Welch and M. J. C. van Gemert, *Optical-Thermal Response of Laser-Irradiated Tissue*. Plenum Press, New York, 1995.
- [27] J. Zhou, J. K. Chen, and Y. Zhang, "Dual-phase lag effects on thermal damage to biological tissues caused by laser irradiation," *Comput. Biol. Med.*, vol. 39, no. 3, pp. 286–293, 2009. DOI: [10.1016/j.combiomed.2009.01.002](https://doi.org/10.1016/j.combiomed.2009.01.002).
- [28] J. Jian and Z. X. Guo, "Thermal interaction of short-pulsed laser focused beams with skin tissues," *Phys. Med. Biol.*, vol. 54, no. 13, pp. 4225–4241, 2009. DOI: [10.1088/0031-9155/54/13/017](https://doi.org/10.1088/0031-9155/54/13/017).
- [29] N. Sharma, R. Kumar, and P. Ram, "Plane strain deformation in generalized thermoelastic diffusion," *Int. J. Thermophys.*, vol. 29, no. 4, pp. 1503–1522, 2008. DOI: [10.1007/s10765-008-0435-8](https://doi.org/10.1007/s10765-008-0435-8).
- [30] L. Brancik, "Programs for fast numerical inversion of Laplace transforms in MATLAB language environment," Proceedings of the 7th Conference MATLAB '99Czech Republic Prague. pp. 2739, 1999.
- [31] X. G. Tian and Y. P. Shen, "Study on generalized magneto-thermoelastic problems by FEM in time domain," *Acta Mech Sinica*, vol. 21, no. 4, pp. 380–387, 2005. DOI: [10.1007/s10409-005-0046-6](https://doi.org/10.1007/s10409-005-0046-6).
- [32] H. H. T, X. G. Tian, and Y. P. Shen, "Two-dimensional generalized thermal shock problem of a thick piezoelectric plate of infinite extent," *Int. J. Eng. Sci.*, vol. 40, no. 20, pp. 2249–2264, 2002.
- [33] D. C. M. Vyas, S. Kumar, and A. Srivastava, "Porous media based bio-heat transfer analysis on counter-current artery vein tissue phantoms: Applications in photo thermal therapy," *Int. J. Heat Mass Trans.*, vol. 99, pp. 122–140, 2016. DOI: [10.1016/j.ijheatmasstransfer.2016.03.106](https://doi.org/10.1016/j.ijheatmasstransfer.2016.03.106).